Landslides (2017) 14:1235–1240
DOI 10.1007/s10346-016-0790-7
Received: 2 September 2016
Accepted: 12 December 2016
Published online: 26 December 2016

Chi-Wen Chen · Takashi Oguchi · Yuichi S. Hayakawa · Hitoshi Saito · Hongey Chen

Relationship between landslide size and rainfall conditions in Taiwan

Abstract This study analyzed the size of 172 rainfall-induced landslides in Taiwan during 2006–2012. Comparing the landslide size with rainfall conditions, this study found that large and deep landslides usually occurred due to long-duration and moderate-intensity rainfall (11.5–31.0 mm/h; 26.5–62.5 h), whereas small and shallow landslides occurred in a wide range of rainfall intensity and duration (8.5–31.0 mm/h; 4.0–62.5 h). This observation is ascribable to the fact that large and deep landslides need a high ground water level caused by a prolonged rainfall. Concerning the area of landslides, their frequency–area distribution correlates well with a power law relation having an exponent of −1.1 ± 0.07, over the range 6.3×10^2 to 3.1×10^6 m^2. The slope of the power law relation for the size–frequency distribution of landslides in Taiwan is lower than those for other areas around the world. This indicates that for the same total area or total number of landslides, the proportion of large landslides is higher in Taiwan than in other areas.

Keywords Landslides · Rainfall · Intensity · Duration · Frequency–area · Power law

Introduction

It is well known that rainfall plays a significant role in triggering landslides in mountainous areas worldwide. The influence of rainfall on landslides differs substantially depending upon landslide dimensions, kinematics, and material involved. Usually, shallow landslides are triggered by high-intensity rainfall within a short duration, while most deep-seated landslides are related with the rainfall duration lasting for a long period (Brunsden 1984; Cannon and Ellen 1985; Wieczorek 1987; Larsen and Simon 1993; Crosta 1998; Polemio and Sdao 1999; Flentje et al. 2000; Trigo et al. 2005). Many studies have also examined landslides in terms of their number, area, and volume. Lumb (1975) found that disastrous events with more than 50 landslides per day occurred when the 24-h rainfall exceeded 100 mm and the 15-day antecedent rainfall exceeded 350 mm in Hong Kong. Dai and Lee (2002) also studied rainfall-induced landslides in Hong Kong and found that the 12-h rolling rainfall is the most important in predicting the number of landslides, but in terms of failure volume, the most important rainfall period seems to be 24 h. Saito et al. (2014) found that rainfall totals appear to be a suitable predictor of landslide volumes mobilized during typhoons and frontal storms in Japan. In terms of the landslide area, it was found that the frequency–area distribution of landslides correlates well with a power law relation (Hovius et al. 2000; Guzzetti et al. 2002; Malamud et al. 2004a, b).

Taiwan represents an area extremely susceptible to landslides because of the steep mountainous topography, complex geological conditions, frequent heavy rainfall, and frequent earthquakes. Thus, many studies have been performed on landslides in Taiwan (Jan and Chen 2005; Chang and Chiang 2009; Lin and Chen 2012). However, these studies typically examined specific events or locations. Chen et al. (2015) established the rainfall intensity (*I*)–duration (*D*) threshold for landslides in Taiwan. A generalized model for reproducing approaches like *I*–*D* schemes is provided by De Luca and Versace (2017), while a methodology to systemically and objectively calibrate, verify, and compare different models is detailed in Formetta et al. (2016). Although it is supposed to be useful for the landslide warning, we cannot estimate the size of impending landslides. Since the size of landslides and the severity of disasters are closely related, it is important to firmly recognize the characteristic of landslide size. Therefore, the objective of this study is to identify dimensional characteristics of landslides associated with rainfall conditions across the whole extent of Taiwan.

Study area

Taiwan is located on a convergent plate boundary between the Eurasian Continental and the Philippine Sea plates, with the Philippine Sea plate moving towards the Eurasian Continental plate at a rate of 80 mm/year (Yu et al. 1997). The subduction of the Philippine Sea plate beneath the Eurasian Continental plate resulted in the formation of an active mountain belt called the Central Range with over 200 peaks higher than 3000 m a.s.l. (Ho 1986; Teng 1990). It is also responsible for frequent large earthquakes and an orogenic uplift rate of about 5 to 7 mm/year (Li 1976; Willett et al. 2003). About 32% of Taiwan is above 1000 m a.s.l. The slope of mountainous areas is mostly between 30° and 50° (Chen et al. 2015).

Taiwan is located between 120° E and 122° E and between 22° N and 25° N, and the boundary between tropical and subtropical monsoon climates is located in the south of Taiwan (Wang and Ho 2002). The average temperature over the Taiwanese lowlands during the wet season (May to October) is above 20 °C, while that during the dry season (November to April) is between 14 and 20 °C. Central and southern Taiwan is mountainous, making the average temperature lower than in other regions of the country (Chen et al. 2015). On average, four typhoons strike Taiwan every year (Wu and Kuo 1999), causing heavy and concentrated rainfall. Annual rainfall over Taiwan averages 2500 mm. However, annual rainfall in mountainous regions can surpass 3000 mm (Shieh 2000). Approximately 60 to 80% of rainfall falls during the wet season (Chen et al. 2015).

Heavy rainfall, steep topography, and high seismicity in Taiwan have contributed to erosion rates of 3 to 7 mm/year (Dadson et al. 2003). Landslides triggered by frequent rainfall and earthquakes represent the primary mechanisms of this erosion and are important for maintaining balance between erosion and uplift (Dadson et al. 2003). Taiwan also has a fragile geological environment, and areas with a high density of geological discontinuity are more prone to landslides (Chen et al. 1999; Chen and Su 2001; Chuang et al. 2009).

Data and methods

Landslide data

This study analyzed 172 landslides caused by heavy rainfall during the 7-year period between 2006 and 2012 (Fig. 1). We

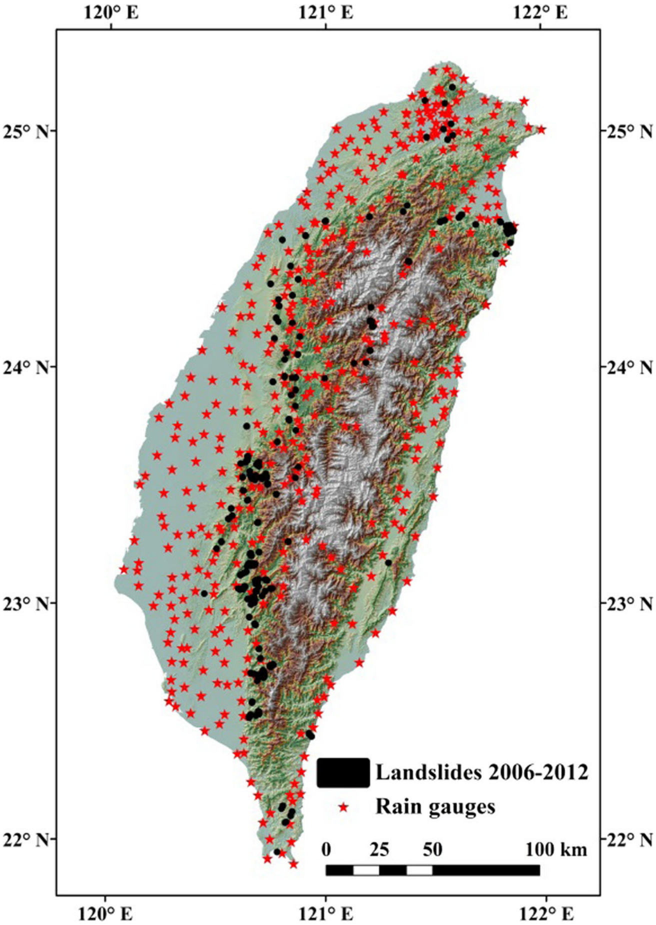

Fig. 1 Distributions of rain gauges and landslides that occurred during 2006–2012 in Taiwan

collected landslide data from the reports of the Soil and Water Conservation Bureau (SWCB) of Taiwan. The SWCB has conducted detailed field surveys when rainfall-induced mass movement disasters such as damage of houses and roads occurred for preventing secondary disasters and quick recovery. The resultant reports contain information on the type, location, and approximate time (accuracy in hour) of each disaster event. They speculate the time based on real-time videos taken at observation stations, the time people informed disasters, and interviews with residents. They investigate the extent of affected areas and the damaged condition of residents and constructions. Types of disaster in these reports are classified into three: landslides, debris flows, and floods. We selected landslides for our analysis because the areal extent of debris flows is difficult to identify on satellite images.

In the dataset used, only a few landslides distributed in very high mountainous areas, because the SWCB only reported landslides, which directly affected residences and infrastructures. Although landslides occur frequently in Taiwan, there is yet no complete inventory with very detailed information. The relatively high integrity and consistency of the data collected by the SWCB indicate that at this moment, the data are the best for analyzing dimensional characteristics of landslides associated with rainfall conditions over Taiwan.

The landslide mapping was conducted using FORMOSA-II images with a resolution of 8 m, which can be previewed at the website of the Center for Space and Remote Sensing Research, Nation Central University, Taiwan (http://earth.csrsr.ncu.edu.tw/CSRSR/QUERY3/QueryScreen.htm). The error of landslide mapping could be negligible because of the use of high-resolution images. After mapping the landslides, we calculated the area of each landslide. Many previous studies have found that the frequency–area distribution of landslides correlates well with a power law relation (Hovius et al. 2000; Guzzetti et al. 2002; Malamud et al. 2004a, b). Differences in the shape of frequency–area distribution between different areas reflect regional characteristics. The frequency–area distribution was obtained using the landslide area data and the probability density function:

$$P(A_L) = \frac{1}{N_{LT}} \frac{dN_L}{dA_l} = CA_L^{-B} \tag{1}$$

where N_{LT} is the total number of landslides, dN_L is the number of landslides with area between A_L and $A_L + dA_L$, C is the scaling constant (intercept), and β is the shape parameter (slope). We also used the robust random sampling method due to its resistance to errors and outliers (Korup et al. 2012; Little and Rubin 2014; Chen et al. 2015). To calculate the probability density, 100 data were randomly sampled, and this was repeated 50 times, allowing us to obtain the mean and standard deviation of C and β in Eq. (1). We set 50 equal-interval bins for the logarithm of landslide area, between the minimum and maximum areas for the 100 data. Then, we calculated the probability density for each bin. If no data exist in a bin of landslide area, we do not calculate the probability density for the bin; the number of such cases is relatively small.

Many previous studies have demonstrated that the frequency–area distribution follows a power law relation but only for medium- to large-scale landslides (>10^3 m^2) (Sugai et al. 1994; Hovius et al. 2000; Guzzetti et al. 2002; Malamud et al. 2004a, b). The distribution from medium to small landslides (close to 10^2 m^2) often shows a deviation from a power law (so-called rollover) (Hovius et al. 2000; Guzzetti et al. 2002; Malamud et al. 2004a, b).

Researchers have investigated the frequency–area relationship of landslides for different areas in the world (Table 1). Fujii (1969) studied landslides caused by heavy rainfall events in Japan and found that the slope of the frequency–area distribution (β) is 1.96. Hovius et al. (1997) obtained β = 2.17 for landslides in New Zealand. Hungr et al. (1999) dealt with rockfalls and rock slides along the main transportation route of southwestern British Columbia and found β = 1.75 ± 0.30. Malamud and Turcotte (1999) noted that β = 1.6 for landslides in the Challana valley, Bolivia; β = 2.0 for the Akaishi Range, central Japan; and β = 2.3 for the Eden Canyon, Alameda, USA. Dai and Lee (2002) analyzed landsides in Hong Kong and found that β = 2.2. Guzzetti et al. (2002) studied two datasets of landslides in central Italy and found that β = 1.5. They then concluded that many landslide inventories satisfy β = 1.5 ± 0.5.

Rainfall data

Taiwan's Central Weather Bureau has installed more than 400 rain gauges with a density of approximately one gauge every 76 km^2 (Fig. 1) that record hourly data. The apparatuses of these rain gauges are the tipping bucket type, which can be used for automated observations. Since rain gauges were not always located close to landslide sites and relatively few rain gauges were distributed in mountainous areas, we selected the nearest five rain gauges for each landslide and conducted a kriging interpolation using the ordinary kriging and the spherical semivariogram model with a variable search radius to estimate rainfall at each landslide location. Many other interpolation methods exist such as the spline and inverse distance weighting (IDW) methods, and different areas require different methods (Tao et al. 2009). However, deciding the best method for an area is quite difficult. For this reason, we chose the kriging interpolation, which is commonly used in Taiwan for the gauged rainfall estimate (Chiang and Chang 2009; Chen et al. 2015). Then, we obtained the hourly rainfall value at the location of each landslide. As is common in Taiwan, one continuous rainfall event was considered to begin when hourly rainfall surpassed 4 mm and to end when hourly rainfall decreased to below 4 mm over the next six consecutive hours (e.g., Chang et al. 2011). We calculated the mean rainfall intensity (I, mm/h), rainfall duration (D, h), and cumulative rainfall (mm) from the beginning of a rainfall event to the time of landslide occurrence. We also examined rainfall totals for 168 h (1 week) before the beginning of rainfall events that triggered landslides.

Results and discussion

Landslide size and rainfall conditions

During 2006–2012, the landslide area was 7.0×10^4 m^2 on average, ranging from 6.3×10^2 to 3.1×10^6 m^2. Most landslides (91.9%) have areas between 10^3 and 10^5 m^2 (Fig. 2). There are two particularly large landslides caused by Typhoon Morakot in 2009 (Fig. 3). The largest one occurred in Jiaxian District, Kaohsiung City, with the area of 3.13×10^6 m^2, mean rainfall intensity of 23.3 mm/h, duration of 57 h, and cumulative rainfall of 1327.3 mm. The second largest one occurred in Wutai Township, Pingtung County, with the area of 2.11×10^6 m^2, mean rainfall intensity of 16.8 mm/h, duration of 29 h, and cumulative rainfall of 485.9 mm. Both are deep-seated landslides deeper than 2 m. Mean rainfall intensity for all landslides ranged from 8.9 to 64.8 mm/h with an average of 20.9 mm/h, and rainfall duration ranged between 2 and 71 h with an average of 33 h. Cumulative rainfall was as low as 60.3 mm and as high as 1738.5 mm with an average of 663.8 mm. Chen et al. (2015) pointed out that antecedent rainfall plays an important role in triggering landslides in Taiwan. The average rainfall total for 168 h before the beginning of rainfall events for the 172 landslides is 142.2 mm, with a wide range from 1.8 to 707.3 mm and a large standard deviation of 160.8 mm. However, no relationship could be found between landslide size and antecedent rainfall (Fig. 4). Therefore, in the following discussion, we focus on rainfall conditions of the latest rainfall event related to landslide size.

Figure 5a shows rainfall conditions of landslides in which the circle size represents the size of landslide area. Large landslides tend to be associated with longer-duration rainfalls. The landslides were classified into three groups with similar landslide numbers, according to the landslide area: (1) <9000 m^2; (2) 9000–24,000 m^2; and (3) >24,000 m^2. The three groups contain 58, 58, and 56 landslides, respectively. Figure 5b shows the density of data distribution of these three groups: the data of group 1 are distributed very widely, but with the increase of landslide area (groups 2 to 3), and data distributions become more centralized at longer-duration rainfalls. This phenomenon is consistent with some previous studies that deep and large slides usually occur only due to long-duration and moderate-intensity storms that provide a high ground water level, soil moisture, and pore water pressure, whereas shallow and small slides that remove only soils over bedrock can occur even by short duration storms (Wieczorek 1987; Larsen and Simon 1993). The results of this study show that when the landslide area is smaller than 9000 m^2, the most concentrated zone of rainfall conditions (darkest color in Fig. 5b) was ranging between 8.5 and 31.0 mm/h of mean intensity and 4.0 and 62.5 h of duration. For the landslides larger than 24,000 m^2, the most concentrated zone of rainfall conditions was ranging between 11.5 and 31.0 mm/h of mean intensity and 26.5 and 62.5 h of duration. Chen et al. (2015) pointed out that the rainfall intensity plays an important role in triggering landslides in Taiwan. Regarding the landslide size, however, rainfall intensities for the three groups are not different too much. On the other hand, rainfall durations for the three groups are quite different. These indicate that rainfall intensity is the key factor to trigger a landslide, while rainfall duration is the key factor to determine the landslide size in Taiwan.

Chen et al. (2015) have also proposed the I–D threshold for landslides in Taiwan, which is also plotted in Fig. 5. The combination of the results of this study together with the I–D threshold

Table 1 Slope of landslide frequency–area distributions

Reference	Area	Number of landslide	Slope (β)
This study	Taiwan	172	1.1 ± 0.07
Hovius et al. (2000)	Eastern Taiwan	1040	1.7
Fujii (1969)	Japan	800	1.96
Hovius et al. (1997)	Alpine fault, New Zealand	4984	2.17
Hungr et al. (1999)	Southwestern British Columbia	1937	1.75 ± 0.30
Malamud and Turcotte (1999)	Challana valley, Bolivia	1130	1.6
	Akaishi Range, central Japan	3243	2.0
	Eden Canyon, Alameda, USA	709	2.3
Dai and Lee (2002)	Hong Kong	2811	2.2
Guzzetti et al. (2002)	Central Italy	21,042	1.5

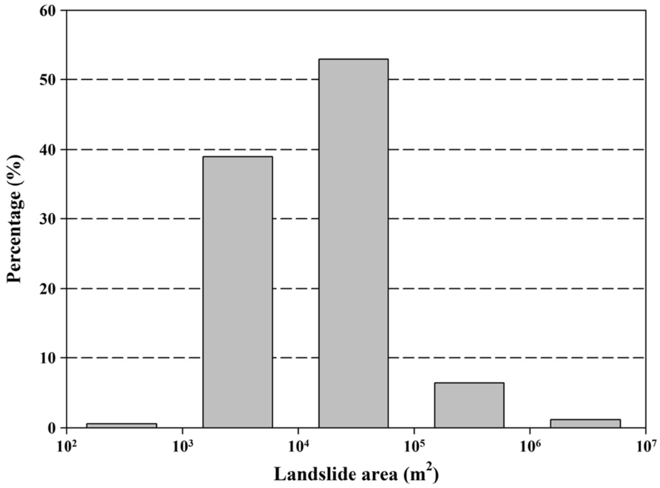

Fig. 2 Distribution of landslide area during 2006–2012

could contribute hugely to the landslide warning. If rainfall conditions exceed the threshold line, it is supposed to have landslide occurrences. Moreover, checking which concentrated zone of the three groups the rainfall condition is located allows us to estimate the possible size of impending landslides.

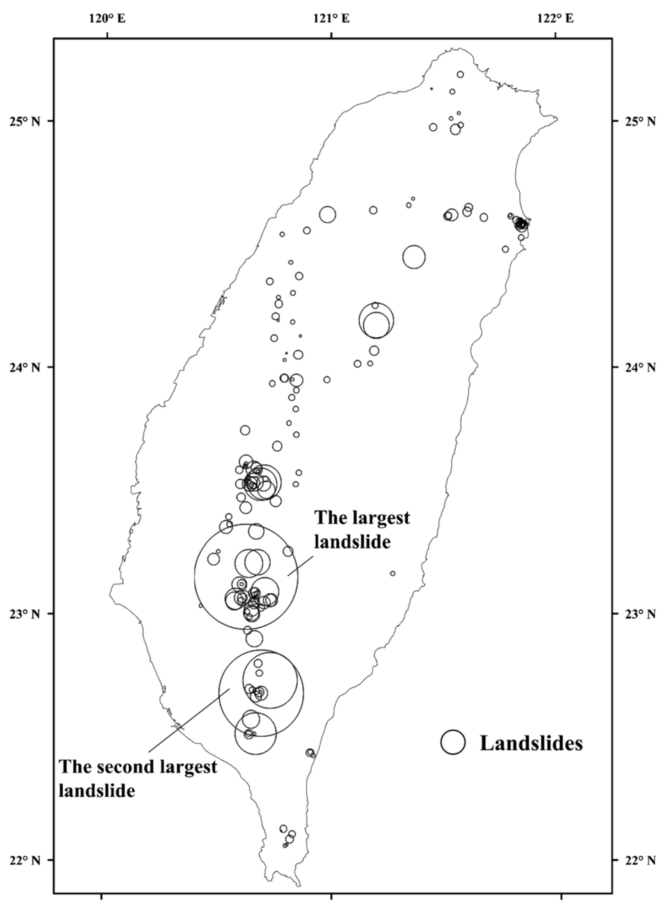

Fig. 3 Distribution of the collected landslides in this study with landslide size (*circle size*)

Frequency and area of landslides

The area of all 172 mapped landslides exhibits a frequency–area distribution that can be described by a power law over more than three orders of area magnitude with a good fit ($R^2 = 0.87$) (Fig. 6):

$$P(A_L) = 787.6(\pm 596.6)A_L^{-1.1(\pm 0.07)}\left(6.3\times 10^2\text{m}^2 < A_L < 3.1\times 10^6\text{m}^2\right) \qquad (2)$$

In this study, the distribution only displayed the segment for medium to large landslides (6.3×10^2 m² < A_L < 3.1×10^6 m²) without a visible rollover (Fig. 6). The SWCB may not have reported small-scale landslides because they focused on the landslides which caused disasters such as the damage of houses or roads.

As mentioned, the landslide frequency–area relationships for different areas in the world have been investigated (Table 1). In this study, β for Taiwan is 1.1 ± 0.07. Hovius et al. (2000) have studied landslides in the Ma-An and Wan-Li catchments, eastern Taiwan, and found that β is 1.7. Both values for Taiwan are much lower than those in the other areas. The lower values for Taiwan indicate that if the same total area or total number of landslides occurred, the proportion of large landslides is higher in Taiwan. It may reflect high-relief topography, complex geology, high cumulative precipitation amounts, and frequent heavy storms in Taiwan that lead to frequent deep and large landslides. The difference in β between eastern Taiwan (Hovius et al. 2000) and the whole of Taiwan (this study) could be related to massive and intact metamorphic and volcanic rocks in the former, which may lower the possibility of large landslides. Figure 3 shows the distribution of the collected landslides in this study with landslide size. It is clear from Fig. 3 that most of the large landslides were concentrated on the southwestern Taiwan and most of the small landslides and some large landslides were distributed in the central, north, and northeastern Taiwan. On the other hand, very few landslides, which were also relatively small size, were distributed in the eastern Taiwan, supporting that β for the eastern Taiwan should

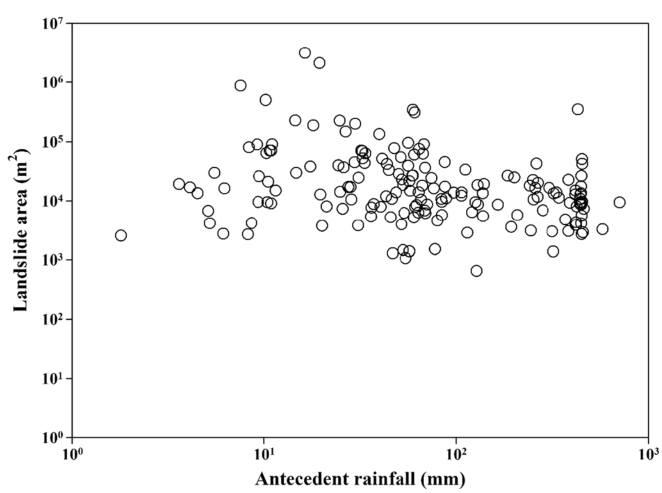

Fig. 4 Relationship between antecedent rainfall and landslide size

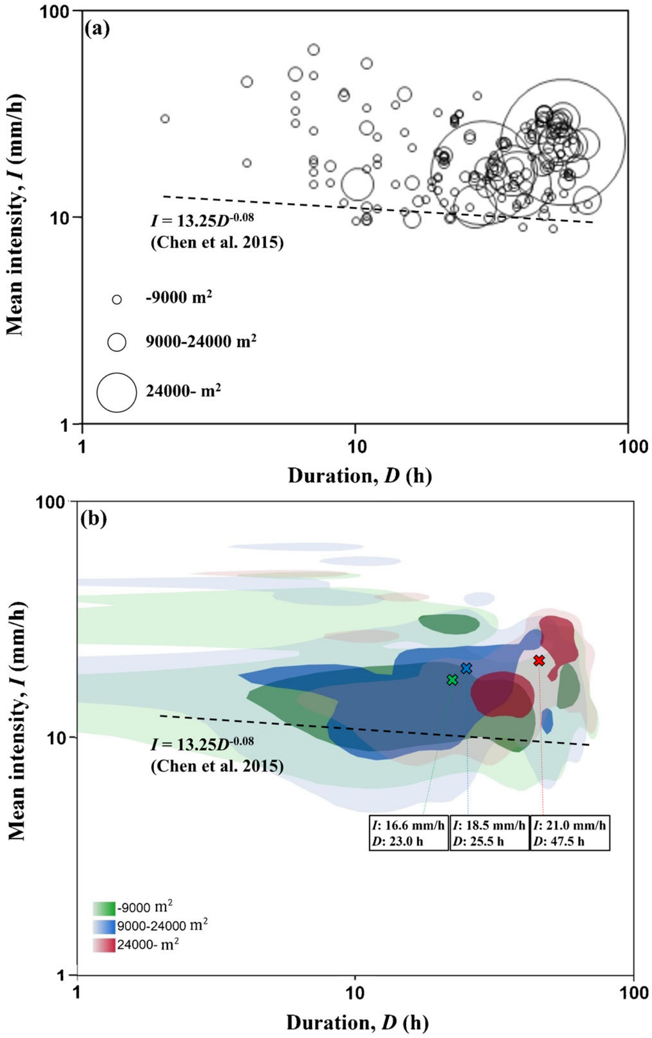

Fig. 5 Rainfall duration–intensity relationship for landslides during 2006–2012. **a** Landslide size and rainfall conditions. *Circle size* represents the size of landslide area. **b** Rainfall conditions for three groups of landslide area. The density map is obtained from the non-parametric density and the area of *darkest color* covering 95% of data. *Cross marks* are median values of *I* and *D* for the three groups. *Dashed line* is the *I*–*D* threshold for landslides in Taiwan proposed by Chen et al. (2015)

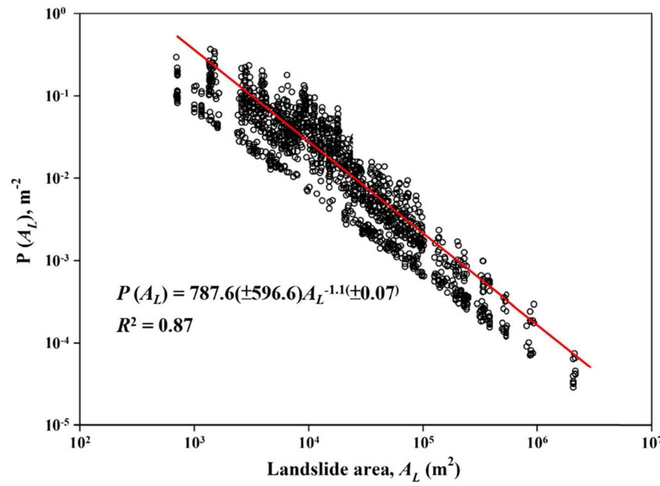

Fig. 6 Log-binned probability density distribution of landslide area in Taiwan

be higher than that for the whole Taiwan. Geological conditions in Taiwan are varying largely by places. Neogene marine and indurated metamorphosed argillaceous sedimentary rocks mainly underlie the western region. Central Taiwan is composed of metamorphic rocks. North and northeastern Taiwan is composed of agglomerate masses of igneous rock fragments, Quaternary sediments, and Neogene marine sedimentary rocks. The majority of the eastern Taiwan consists of Paleogene metamorphic complex, volcanic arc sediments, orogenic sediments, and a subduction–collision complex (Ho 1988). The differences in landslide size and distribution between different parts of Taiwan may be contributed to the various geological conditions across Taiwan. More studies should be conducted in the future for analyzing the effect of geological conditions on landslide size and distribution.

Conclusions

The areas of 172 landslides were mapped using FORMOSA-II images. We found that large and deep landslides usually occurred due to long-duration and moderate-intensity rainfall, whereas small and shallow landslides occurred in a wide range of rainfall conditions. Shallow landslides can occur even during a short-duration rainfall event because flushing surface materials is easier, whereas deep landslides need a high groundwater level, soil moisture, and pore water pressure caused by a prolonged rainfall. The frequency–area correlation of the landslides in Taiwan is expressed by a power law relation having an exponent of −1.1 ± 0.07. This exponent value is higher than those for other areas around the world, indicating that the proportion of large landslides is exceptionally high in Taiwan. This may be because Taiwan is characterized by high-relief topography, complex geology, high cumulative precipitation amounts, and frequent heavy storms.

Acknowledgements

We would like to thank the Typhoon and Flood Research Institute (TTFRI) and the Soil and Water Conservation Bureau (SWCB) of Taiwan for providing rainfall data and information on landslides. We would also like to thank the Center for Space and Remote Sensing Research, National Central University, for providing satellite images. The authors acknowledge Dr. Naoto Takahata in the Atmosphere and Ocean Research Institute, University of Tokyo, for his inspiring ideas of presenting our data.

References

Brunsden D (1984) Mudslides. In: Brunsden D, Prior DB (eds) Slope instability. Wiley, London, pp. 363–418

Cannon SH, Ellen SD (1985) Rainfall conditions for abundant debris avalanches, San Francisco Bay region, California. Calif Geol 38:267–272

Chang CW, Lin PS, Tsai CL (2011) Estimation of sediment volume of debris flow caused by extreme rainfall in Taiwan. Eng Geol 123:83–90

Chang K, Chiang S (2009) An integrated model for predicting rainfall-induced landslides. Geomorphology 105:366–373
Chen CW, Saito H, Oguchi T (2015) Rainfall intensity–duration conditions for mass movements in Taiwan. Progr Earth Planet Sci 2:1–13
Chen H, Chen RH, Lin ML (1999) Initiative anatomy of Tungmen debris flow, eastern Taiwan. Environ Eng Geosci 5:459–473
Chen H, Su DI (2001) Geological factors for hazardous debris flow in Hoser, central Taiwan. Environ Geol 40:1114–1124
Chiang SH, Chang KT (2009) Application of radar data to modeling rainfall-induced landslides. Geomorphology 103:299–309
Chuang SC, Chen H, Lin GW, Lin CW, Chang CP (2009) Increase in basin sediment yield from landslides in storms following major seismic disturbance. Eng Geol 103:59–65
Crosta G (1998) Regionalization of rainfall thresholds: an aid to landslide hazard evaluation. Environ Geol 35:131–145
Dadson SJ, Hovius N, Chen H, Dade WB, Hsieh ML, Willett SD, Hu JC, Horng MJ, Chen MC, Stark CP, Lague D, Lin JC (2003) Links between erosion, runoff variability and seismicity in the Taiwan orogeny. Nature 426:648–651
Dai FC, Lee CF (2002) Landslide characteristics and slope instability modeling using GIS, Lantau Island, Hong Kong. Geomorphology 42:213–228
De Luca DL, Versace P (2017) A comprehensive framework for empirical modeling of landslides induced by rainfall: the generalized FLaIR model (GFM). Landslides (article in press)
Flentje PN, Chowdhury RN, Tobin P (2000) Management of landslides triggered by a major storm event in Wollongong, Australia. In: Wieczorek GF, Naeser ND (eds) Proceedings of the II International Conference on Debris-Flow Hazards Mitigation, Mechanics, Prediction and Assessment, Balkema, Rotterdam, pp 479–487
Formetta G, Capparelli G, Versace P (2016) Evaluating performance of simplified physically based models for shallow landslide susceptibility. Hydrol Earth Syst Sci 20:4585–4603
Fujii Y (1969) Frequency distribution of landslides caused by heavy rainfall. Journal Seismological Society Japan 22:244–247
Guzzetti F, Malamud BD, Turcotte DL, Reichenbach P (2002) Power-law correlations of landslide areas in central Italy. Earth Planet Sc Lett 195:169–183
Ho CS (1986) A synthesis of the geologic evolution of Taiwan. Tectonophysics 125:1–16
Ho CS (1988) An introduction to the geology of Taiwan, explanatory text of the geologic map of Taiwan. Central Geological Survey, the Ministry of Economic Affairs, Taipei
Hovius N, Stark CP, Allen PA (1997) Sediment flux from a mountain belt derived by landslide mapping. Geology 25:231–234
Hovius N, Stark CP, Hao-Tsu C, Jiun-Chuan L (2000) Supply and removal of sediment in a landslide-dominated mountain belt: Central Range, Taiwan. J Geol 108:73–89
Hungr O, Evans SG, Hazzard J (1999) Magnitude and frequency of rock falls and rock slides along the main transportation corridors of southwestern British Columbia. Can Geotech J 36:224–238
Jan CD, Chen CL (2005) Debris flows caused by Typhoon Herb in Taiwan. In: Jakob M, Hungr O (eds) Debris flow hazards and related phenomena. Springer, Berlin Heidelberg, pp. 539–563
Korup O, Görüm T, Hayakawa Y (2012) Without power? Landslide inventories in the face of climate change. Earth Surf Proc Land 37:92–99
Larsen M, Simon A (1993) A rainfall intensity–duration threshold for landslides in a humid-tropical environment: Puerto Rico. Geogr Ann A 75:13–23
Li YH (1976) Denudation of Taiwan island since the Pliocene epoch. Geology 4:105–107
Lin GW, Chen H (2012) The relationship of rainfall energy with landslides and sediment delivery. Eng Geol 125:108–118
Little RJ, Rubin DB (2014) Statistical analysis with missing data. Wiley, New York
Lumb P (1975) Slope failures in Hong Kong. Q J Eng Geol Hydroge 8:31–65
Malamud BD, Turcotte DL (1999) Self-organized criticality applied to natural hazards. Nat Hazards 20:93–116
Malamud BD, Turcotte DL, Guzzetti F, Reichenbach P (2004a) Landslide inventories and their statistical properties. Earth Surf Proc Land 29:687–711
Malamud BD, Turcotte DL, Guzzetti F, Reichenbach P (2004b) Landslides, earthquakes, and erosion. Earth Planet Sc Lett 229:45–59
Polemio M, Sdao F (1999) The role of rainfall in the landslide hazard: the case of the Avigliano urban area (Southern Apennines, Italy). Eng Geol 53:297–309
Saito H, Korup O, Uchida T, Hayashi S, Oguchi T (2014) Rainfall conditions, typhoon frequency, and contemporary landslide erosion in Japan. Geology 42:999–1002
Shieh SL (2000) User's guide for typhoon forecasting in the Taiwan area (VIII). Central Weather Bureau, Taipei
Sugai T, Ohmori H, Hirano M (1994) Rock control on magnitude–frequency distribution of landslides. Transactions Japanese Geomorphological Union 15:233–251
Tao T, Chocat B, Liu S, Xin K (2009) Uncertainty analysis of interpolation methods in rainfall spatial distribution—a case of small catchment in Lyon. J Environ Prot 1:50–58
Teng LS (1990) Geotectonic evolution of late Cenozoic arc-continent collision in Taiwan. Tectonophysics 183:57–76
Trigo RM, Zêzere JL, Rodrigues ML, Trigo IF (2005) The influence of the North Atlantic Oscillation on rainfall triggering of landslides near Lisbon. Nat Hazards 36:331–354
Wang B, Ho L (2002) Rainy season of the Asian-Pacific summer monsoon. J Clim 15:386–398
Wieczorek GF (1987) Effect of rainfall intensity and duration on debris flows in central Santa Cruz Mountains, California. Rev Eng Geol 7:93–104
Willett SD, Fisher D, Fuller C, Yeh EC, Lu CY (2003) Erosion rates and orogenic wedge kinematics in Taiwan inferred from apatite fission track thermochronometry. Geology 31:945–948
Wu CC, Kuo YH (1999) Typhoons affecting Taiwan: current understanding and future challenges. B Am Meteorol Soc 80:67–80
Yu SB, Chen HY, Kuo LC (1997) Velocity field of GPS stations in the Taiwan area. Tectonophysics 274:41–59

C. Chen · T. Oguchi · Y. S. Hayakawa · H. Saito
Center for Spatial Information Science,
University of Tokyo,
5-1-5 Kashiwanoha Kashiwa, Chiba, 277-8568, Japan

C. Chen (✉) · H. Chen
National Science and Technology Center for Disaster Reduction,
No. 200, Sec. 3, Beixin Road, Xindian District, New Taipei City, Taiwan
e-mail: kevin4919@gmail.com

H. Saito
College of Economics,
Kanto Gakuin University,
1-5-1 Mutsuura-higashi, Yokohama, Kanagawa 236-8501, Japan

H. Chen
Department of Geosciences,
National Taiwan University,
No. 1, Sec. 4, Roosevelt Road, Taipei, Taiwan